



## Review

## Biomedical coatings on magnesium alloys – A review

H. Hornberger<sup>a,\*</sup>, S. Virtanen<sup>b</sup>, A.R. Boccaccini<sup>a</sup><sup>a</sup> Institute of Biomaterials (WW7), Department of Materials Science and Engineering, Friedrich-Alexander-University Erlangen-Nürnberg, Cauerstraße 6, D-91058 Erlangen, Germany<sup>b</sup> Institute for Surface Science and Corrosion (LKO, WW4), Department of Materials Science and Engineering, Friedrich-Alexander-University Erlangen-Nürnberg, Martensstrasse 7, D-91058 Erlangen, Germany

## ARTICLE INFO

## Article history:

Received 13 October 2011

Received in revised form 6 April 2012

Accepted 10 April 2012

Available online 14 April 2012

## Keywords:

Magnesium alloy

Biodegradable materials

Coatings

Conversion

Deposition

## ABSTRACT

This review comprehensively covers research carried out in the field of degradable coatings on Mg and Mg alloys for biomedical applications. Several coating methods are discussed, which can be divided, based on the specific processing techniques used, into conversion and deposition coatings. The literature review revealed that in most cases coatings increase the corrosion resistance of Mg and Mg alloys. The critical factors determining coating performance, such as corrosion rate, surface chemistry, adhesion and coating morphology, are identified and discussed. The analysis of the literature showed that many studies have focused on calcium phosphate coatings produced either using conversion or deposition methods which were developed for orthopaedic applications. However, the control of phases and the formation of cracks still appear unsatisfactory. More research and development is needed in the case of biodegradable organic based coatings to generate reproducible and relevant data. In addition to biocompatibility, the mechanical properties of the coatings are also relevant, and the development of appropriate methods to study the corrosion process in detail and in the long term remains an important area of research.

© 2012 Acta Materialia Inc. Published by Elsevier Ltd. All rights reserved.

## 1. Introduction

Magnesium is the lightest metal, which exhibits a high strength to weight ratio, good thermal and electrical conductivity, excellent vibration and shock absorption, a high damping capacity and electromagnetic shield performance [1–4]. The main disadvantage of Mg and Mg alloys is that they are prone to corrosion; magnesium is one of the most electrochemically active metals. In addition, the wear resistance of Mg and Mg alloys is not very high. Due to this a broad range of coating systems are being developed to overcome these weaknesses for numerous applications [5,6].

The low corrosion resistance of Mg makes Mg alloys appropriate candidates for degradable biomaterials due to their biocompatibility combined with outstanding physical and mechanical properties [7–9], e.g. in comparison with polymers. Magnesium ions are needed in the human body for physiological functions, with consumption lying in the range 250–500 mg day<sup>-1</sup>. About 20 g of Mg is always present in the average 70 kg human body; the toxic dose is unknown. Magnesium and its alloys have been studied as implant materials for numerous medical applications since 1878, which has been discussed in a history review by Witte [10]. However, commercial medical products are still not available. Up to 1980 magnesium materials were generally expensive to

produce, the possible processing routes and the resulting mechanical properties were limited, and many unsolved problems related to the low corrosion resistance existed. Due to the introduction of water-cooled cars and the increased requirements for corrosion resistant alloys the use of Mg alloys in the automobile industry ceased [11]. During the 1990s, these low density materials again became very attractive for transportation applications because of the fuel saving benefits obtainable, however, the relevant knowledge for industrial application was still incomplete [2]. This has led to extensive evaluation of the potential use of magnesium in transportation systems, but up to now tangible applications have been limited, e.g. in aircraft components [1,2]. Nowadays there are new expectations for a variety of applications of Mg alloys as the magnesium production technology is now highly developed.

There is a need of a new generation of biomaterials for innovative implants and tissue scaffolds which should be able to stimulate the healing responses of injured tissues at the molecular level [12–15]. In many cases the body needs only the temporary presence of an implant or device, in which case materials exhibiting biodegradability represent a better approach than stable and inert ones. The ideal biodegradable material, for example in bone regeneration strategies (polymer, ceramic, metal or composite), should provide adequate mechanical fixation, complete degradation once no longer needed, and complete replacement by new bone tissue.

Biodegradable polymers are the materials of choice in several applications, including surgical sutures, antibacterial coatings,

\* Corresponding author.

E-mail address: [helga.hornberger@ww.uni-erlangen.de](mailto:helga.hornberger@ww.uni-erlangen.de) (H. Hornberger).

drug delivery systems, fixation devices and tissue replacement components. Mg alloys present a promising alternative to biodegradable polymers due to their ability for degradation combined with appropriate mechanical properties (usually superior to those of polymers) as well as good biocompatibility. To date magnesium and its alloys have mainly been studied in the development of cardiovascular stents, bone fixation materials, and porous scaffolds for bone repair [8–10].

The main limitation to the application of magnesium alloys as medical implant materials is their corrosion behaviour. Corrosion is too rapid even for a biodegradable material and, additionally, it is not homogeneous, due to a strong tendency for localized corrosion exhibited by Mg alloys. Although galvanic contact corrosion with other conducting materials in a device can be avoided, most impurities or secondary phases enriched with alloying elements in the microstructure have destructive effects, due to internal galvanic corrosion [16]. Another issue is the formation of hydrogen during corrosion: if evolution of the gas is too rapid it cannot be absorbed and a balloon effect takes place. In addition to gas liberation during Mg alloy corrosion, an alkaline pH shift in the vicinity of the corroding surface is also of concern for medical applications.

There are generally two possible ways to improve the corrosion behaviour of Mg and Mg alloys:

- (i) tailor the composition and microstructure, including the grain size [17,18] and texture [19] of the base material, not only through alloying [20] but also through the development of optimized manufacturing methods and the availability of suitable raw materials [21];
- (ii) carry out surface treatments or form coatings [5], which produce protective ceramic, polymer or composite layers.

Although some promising techniques related to both areas have been studied in recent years, further in-depth systematic research is still needed [6]. As alloying of Mg is challenging due to the low solubility of many elements in Mg, coatings are of high significance, and a very attractive way to improve corrosion resistance. Most coatings for Mg alloys described in the literature have not been developed for medical applications, and no commercial products are available in the biomedical devices sector. The main commercial application of the coatings so far has been to improve corrosion resistance or wear resistance, for example of components in aircraft. In some cases the coatings are used for decorative purposes, for example in the mobile phone industry.

The focus of this review concerns the development of biocompatible and biodegradable coatings for Mg and Mg alloys, with the intent of reducing and controlling the corrosion rate and increasing their initial biocompatibility. There has been increasing interest in these coatings since the need for their development was initially discussed [22], as demonstrated by the remarkable increase in the number of publications on this subject in the last few years.

## 2. Coatings for magnesium alloys

Generally coatings can be divided into two classes: conversion coatings and deposited coatings. Conversion coatings are in situ grown coatings which are formed by specific reactions between the base material and the environment [23]. Typically the metallic substrate surfaces are converted during a chemical or electrochemical process into an oxide layer. Related to the original metal surface, the oxide layer grows inwards and outwards at the same time, the geometry of the component therefore changes. The produced layers are inorganic and show ceramic like character. Deposited coatings consist mostly of organic based materials. These

organic coatings are well known in, for example, varnishing in the automotive industry [24]. For Mg alloys, however, a special surface treatment prior to the application of an organic coating is necessary, due to the high surface alkalinity [25]. The surface treatment usually leads to a conversion layer. Deposited coatings can be obtained by numerous techniques to be discussed in this review. For biomedical applications coatings should possess, besides corrosion protection, other functions, such as an enhancement of biocompatibility or osseointegration in the case of orthopaedic applications, bioactivity, antibiotic ability, or local drug delivery ability. Moreover, the coatings should enable biodegradation at a desired rate, and hence they should offer only a limited barrier function.

### 2.1. Conversion coatings

#### 2.1.1. General aspects

An overview of the different techniques used for developing conversion coatings on Mg and Mg alloy substrates is shown in Fig. 1. Conversion coatings arise in a complex interaction of metal dissolution and precipitation, usually during treatments in aqueous solutions. The chemical conversion layers are obtained by immersion of substrates in a bath and show, besides magnesium oxide and magnesium hydroxide, mixtures of other metal oxides and hydroxides, which arise from the dissolved ions in the bath. As conversion coatings are grown in situ adhesion to the substrate is generally very good. Such conversion coatings represent an effective way to increase the corrosion resistance of magnesium alloys or, as a pre-treatment, to improve the adhesion of a final deposited coating [26]. As a pre-treatment conversion coatings perform as a coupling agent or adhesive layer for subsequently deposited organic coatings. In addition to wet chemical immersion methods it is possible to produce oxidation processes by atmospheric and temperature effects. During anodization magnesium substrates are also immersed in a conversion electrolyte, then the components are electrically connected to a power supply and a voltage typically up to 100 V is applied [27]. Plasma electrolytic oxidation (PEO) is a special technique which works with high voltages at the breakdown potential [27–29].

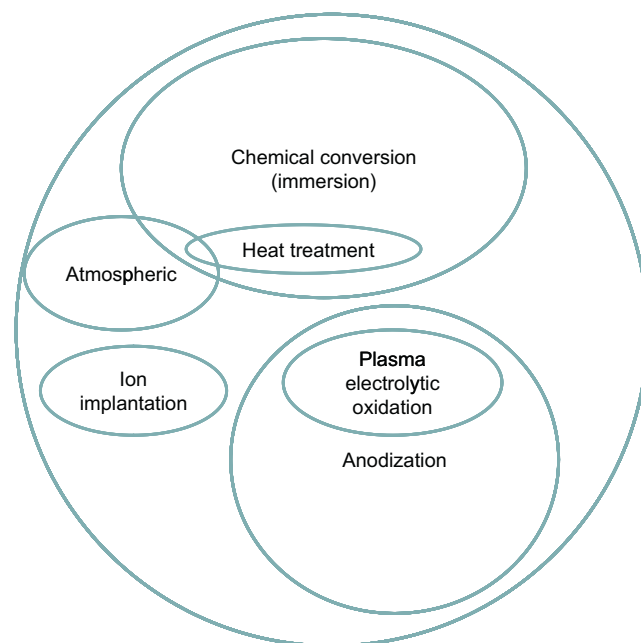


Fig. 1. Schematic diagram showing conversion coatings.

### 2.1.2. Passivation

When Mg alloys are exposed to the ordinary environment a film consisting of magnesium oxide is formed on the surface, atmospheric humidity being sufficient to generate magnesium hydroxide, and storage in air produces in addition carbonate in the layer. The protection provided by this film is limited and it does not show the same protective ability and stability as oxide films that form in the atmosphere on, for instance, aluminium or titanium alloys [30]. Typically the surface layer on Mg alloys is unstable and breaks away because the crystalline lattice is easily cleaved. The layers have a thickness of some nanometres [31–33]. The structure of this layer was studied by Santamaria et al. [32] in detail using X-ray photoelectron spectroscopy (XPS) and photocurrent spectroscopy (PCS), which indicated that the layer consists of an inner MgO layer of 2.5 nm and an outer Mg(OH)<sub>2</sub> layer of 2.2 nm. Seyeux et al. [33] found indications of the existence of MgH<sub>2</sub> within this layer. Asami et al. [31] found a clear correlation between the composition and the thickness of the air formed surface coating, in that hydration led to thickening of the film. Liu et al. [34] found an increased oxide thickness of 10 nm for Al–Mg intermetallics compared with other studies on pure magnesium.

The Mg(OH)<sub>2</sub> layer increases in thickness by several nanometres during immersion in water, whereas the inside MgO layer retains a constant thickness [32]. In the case of alloys Song et al. [16] developed a three layer model for air formed films immersed in NaCl solution, based on electrochemical measurements. Thermal treatment is necessary to significantly thicken the oxide layer. Thermal oxidation was shown to be a simple method of increasing the initial corrosion protection, e.g. to avoid the hydrogen burst due to corrosion reactions during initial immersion in simulated body fluid (SBF) [35]. In this study WE43 alloy samples were oxidized at 500 °C in air for various times between 1 and 168 h. The increased corrosion resistance in this case was attributed to the formation of a thickened Y<sub>2</sub>O<sub>3</sub> layer on the surface of the alloy upon thermal oxidation.

Immersion in a solution with a stable pH of 11 or higher is required for the formation of a passive layer on Mg [36]. A simple approach to protect magnesium is therefore passivation in a NaOH solution to form a layer of MgO/Mg(OH)<sub>2</sub>. Cell culture tests, however, showed that even though the oxide/hydroxide passive layer can reduce the initial surface reactivity when in contact with cell culture medium, it was not stable [37]. Since cell culture medium contains Cl<sup>-</sup>, with the pH buffered to 7.4, the passive film on Mg can be expected to dissolve or undergo localized breakdown. This study moreover showed that cell death on pure magnesium samples without treatment occurs within 1 day, whereas surface passivation enables survival of a number of cells on Mg. However, cell densities were found to be reduced on Mg samples even with prior passivation treatments, compared with glass substrates used as a reference. Cell death was thought to be related to the ongoing corrosion of Mg in cell culture medium, leading to a pH increase. This is in line with recent studies which have indicated that cell culture tests do not provide enough volume to compensate for the high concentration of Mg<sup>2+</sup> ions or the alkaline pH shift in solution, and may hence not be appropriate for testing resorbable materials [38].

Ng et al. [39] performed hydrothermal treatments on pure magnesium to produce a layer of Mg(OH)<sub>2</sub> as a pre-treatment to promote adhesion to a final organic coating. The corrosion resistance was found to be increased due to this layer. The layer was about 170 μm thick and showed a plate-like structure. That is well beyond the typical passive layer of several nanometres.

Simple passivation treatments by soaking Mg and Mg alloy samples in NaOH solution can therefore provide protection during the initial phases of corrosion in other environments. The protective ability, however, is limited, as chlorides, sulphates or other

hydrophilic substances promote corrosion by rapidly destroying the passive film. In the presence of chlorides the corrosion mechanism is supported by the formation of MgCl<sub>2</sub> [40] and by pit nucleation [41].

### 2.1.3. Chemical conversion layers

Chemical conversion coatings include, in addition to magnesium oxide/hydroxide, mixtures of other oxides and hydroxides formed from the bath solution. Chromate coatings show effective corrosion protection for Al and Mg alloys. However, due to an EU regulation of 2007 for the automotive sector, compounds containing Cr(VI) have been banned from use in chemical conversion baths, and it was necessary to develop environmentally friendly replacements for chromate coatings. In the context of biomedical applications Cr(VI)-containing conversion coatings are not feasible, as leaching of carcinogenic chromate from the coatings can take place (for corrosion protection release of Cr(VI) from the Cr<sub>2</sub>O<sub>3</sub> coating is required).

Many metal phosphates are used as anti-corrosive films for magnesium alloys, since they are insoluble in water and have high temperature resistance and chemical stability. Over recent decades alternative chromate-free coatings have been subjected to intensive study, not only magnesium phosphate [42–44], but also zinc phosphate [45,46], manganese phosphate [47–50], aluminium-containing hydrotalcite [51–53], zirconium oxide [54] and others. The corrosion behaviour of those layers strongly depends on the electrolyte composition of the conversion bath and on the alloy substrate. Typically, the resulting layer thicknesses are <10 μm [50,55].

A general overview of chemical conversion coatings in technical applications has been given by Chen et al. [56], showing that the coating performance relies heavily on appropriate pre-treatments to functionalize the surface. Chemical conversion coatings are still a matter of intensive research as they are a cost-effective method to increase the use of Mg alloys in a broad range of applications, including the biomedical field. For biomedical applications biodegradable coatings such as calcium phosphate and fluoride-containing layers are the most interesting in this category.

**2.1.3.1. Chemical conversion: calcium phosphate-containing layers.** Calcium phosphate-containing layers are of special interest for biomedical application in bone substitution and orthopaedic materials, due to the formation of a hydroxyapatite (HA) layer, which is similar to the mineral phase of bone. The most important requirement is adjustment of the phases during processing. The resulting layers are often mainly amorphous, but they contain some crystallized HA and also other calcium phosphate phases. Conversion coatings are formed in a direct reaction with the base material, and, as a result, Mg compounds will always be detected in these coatings.

One approach to obtain calcium phosphate-containing coatings is immersion in SBF; this process is often termed bio-mimetic if carried out at 37 °C and a pH of 7.4. Various compositions of surface layers depending on the bath solution were reported by Rettig and Virtanen [57], including amorphous carbonated calcium/magnesium phosphate layers which formed after immersion in SBF solution for 5 days. Those layers had a thickness of ≥20 μm, and were seen to be highly permeable [57,58]. In a related investigation Lorenz et al. [37] showed the formation of a mixed calcium/magnesium phosphate layer on pure magnesium on soaking in SBF solution, which initially increased the survival of human HeLa cells compared with Mg surfaces after simple soaking in NaOH solution. An interesting aspect of this work concerns an investigation of the surface roughness, which was increased by the SBF treatment. It should be mentioned that different compositions of SBF solution have been developed [57,59], and, since calcium phosphate

formation is a precipitation process depending on the solubility of the calcium phosphate phase formed, different types of coating can be formed using different SBF solutions. Jo et al. [60] produced Ca and P containing layers via immersion into SBF, and included various oxidizing pre-treatments. Surface treated samples were tested in direct contact with MC3T3-E1 cells and showed a significant improvement in cell attachment.

A number of studies have been carried out to control the phase composition of calcium phosphate coatings. For example, Hiromoto and Yamamoto [61] synthesized HA on a magnesium surface without pre-treatment by immersion in a solution of Ca-EDTA,  $\text{KH}_2\text{PO}_4$  and NaOH at various pH values at 110 °C, the immersion times varied between 6 and 24 h to control the coating thickness. Using polarization techniques the authors showed that the corrosion resistance increased with growing coating thickness, indicated by a reduction in the corrosion current density. Phase analysis of the coatings showed that besides HA other phases, including Mg-containing phases, were present, even though an attempt was made to suppress the formation of magnesium hydroxide and magnesium phosphate by adding high concentrations of Ca ions to the conversion solution.

A study by Gray-Munro and Strong [62] produced a coating on Mg alloyed with Al and Zn in three steps. The pre-treatment involved passivation via immersion in NaOH solution followed by a thermal treatment, in order to reduce corrosion during the following SBF conversion coating process. The focus of this study was characterization of the coating phases. Again, the coating showed, besides calcium phosphate, Mg phases, and it was mostly amorphous, containing only small amounts of crystallized HA. The results imply that nucleation and growth of HA were catalysed by dissolution of Mg from the substrate. Coatings of <3  $\mu\text{m}$  thickness exhibited many cracks, as revealed by SEM analysis: after 3 h immersion the coating was seen to contain cracks due to corrosion, while the thicker coatings after 24 and 96 h showed cracking due to dehydration.

Chen et al. [63] used a calculated equilibrium diagram to obtain a stable HA coating using a calcium nitrate and sodium phosphate solution. Nevertheless, a post-treatment in alkaline solution was necessary to develop a HA component within the coating. The HA-Mg(OH)<sub>2</sub> coating produced improved the corrosion resistance of the Mg substrate.

A study by Xu et al. [64] included in vitro and in vivo tests on Mg-Mn-Zn alloy substrates. After an alkaline pre-treatment followed by immersion in calcium phosphate solution coatings containing mainly  $\text{CaHPO}_4 \cdot 2\text{H}_2\text{O}$  (DCPD) and small quantities of  $\text{Mg}^{2+}$  and  $\text{Zn}^{2+}$  were fabricated. The surfaces appeared to be porous. The study compared samples with and without a calcium phosphate coating using titanium as a reference. The number of cells on the coated surfaces was similar to the number of cells on the reference, which were significantly higher than on surfaces without a coating. For in vitro studies 18 rabbits were used to compare the implantation of coated and uncoated Mg alloy samples. A study of the optical cell density on histological cross-sections showed that the coating disappeared after 4 weeks, after which time period the coated and uncoated samples showed no significant differences. This study indicates that good results can be achieved by not only adjusting the calcium phosphate phases but also by using alloys instead of pure magnesium as the substrate.

Yang et al. [65] produced amorphous calcium/magnesium phosphate coatings on AZ31 alloy samples with no pre-treatment but a thermal post-treatment at 300 °C after immersion in sodium phosphate, sodium carbonate and calcium nitrate solution. The samples, coated and uncoated, as well as a degradable polymer as a control group, were implanted into nine rabbits. After 8 weeks the coated implants showed a slower biodegradation rate, confirming the positive effect of the phosphate coatings.

**2.1.3.2. Chemical conversion: fluoride-containing layers.** Fluoride-containing biomedical coatings on Mg alloys have been studied by several authors [66–69]. Fluoride containing coatings on Mg alloys are known from fluoride-based acid pickling [70], which is applied as a pre-treatment to remove contamination from the surface. The coating procedure is usually performed by immersion of Mg or Mg alloy substrates in 40% or 48% hydrofluoric acid. Due to the low solubility of  $\text{MgF}_2$ , this leads to the rapid formation of a conversion layer containing  $\text{MgF}_2$  on the substrate. As  $\text{MgF}_2$  will slowly dissolve when the samples are removed from concentrated HF no permanent protective effect can be achieved. However, a significant increase in the corrosion resistance of Mg and Mg alloy samples is usually observed due to the fluoride-containing coating on the surface. Chiu et al. [67] used pure magnesium as a substrate and obtained uniform dense coatings of 1  $\mu\text{m}$  thickness. The phase analysis showed that the resulting layer contained amorphous phases, tetragonal  $\text{MgF}_2$ , some  $\text{Mg(OH)}_2$  and high concentrations of C. Corrosion studies, i.e. immersion tests and polarization and impedance spectroscopy, were performed in Hanks solution. Carboneras et al. [66] studied pure Mg, cast and produced by powder metallurgy, as well as the Mg alloy AZ31 and confirmed, by immersion tests for 11 days and impedance spectroscopy in cell culture medium, that HF treatment is an effective way to slow down the corrosion rate.

Witte et al. [68] studied a rare earth-containing Mg alloy, LAE442, in vivo. Two groups of 20 rabbits were used, one group with fluoride-containing coated implants and one group with uncoated implants. The alloys of both groups showed low corrosion rates and no subcutaneous gas cavities. However, the coating was seen to delay corrosion, and to disappear after 4 weeks implantation. The  $\text{MgF}_2$  coating seemed to irritate the local synovial tissue during dissolution. Pitting corrosion occurred after breakdown of the coating. The results indicate that greater pitting corrosion took place on the coated than on the uncoated alloy.

A study by Seitz et al. [69] indicated that the protective effect against corrosion of  $\text{MgF}_2$  coatings depends on the alloy composition. In order to determine the corrosion resistance immersion tests in SBF were carried out using an orbital shaker to produce flowing conditions, and the corrosion rate was measured as weight and volume loss. After the immersion tests the coated samples corroded more homogeneously than uncoated samples. For a coated Mg-Li-Al-Nd alloy the corrosion process was delayed by up to 20 days, however, for a Mg-Nd alloy the coatings had no significant effect on the degradation rate. SEM revealed 1.6  $\mu\text{m}$  thick coatings having fine cracks. Although Seitz et al. [69] obtained differing results compared with other related studies [66–68], the overall result was an improvement in corrosion resistance/behaviour due to the presence of the coating. The corrosion test applied (immersion in flowing medium) possibly led to results which are not comparable with static immersion tests. Flowing medium tests seek to simulate blood flow in the vasculature, whereas the in vivo tests by Witte et al. [68] were performed in tissue. Additionally, it is not known whether all or only some fluoride layers have microcracks.

#### 2.1.4. Anodization

**2.1.4.1. Basics of the anodization process.** The classical electrochemical conversion is termed anodization. The coating thicknesses can range from 5 to 200  $\mu\text{m}$  [71]. Typically, anodic oxide layers grow according to the high field model [72], leading to a direct dependence of the oxide thickness on the applied voltage. For metals and alloys with barrier type anodic oxide films blocking electron conduction under anodic polarization an anodization can be carried out at high voltages in aqueous solution. Therefore, thick oxides can be grown on, for instance, Al, Ti and Ta. For metals with conducting oxide layers anodization is limited to voltages below that at which water dissociates with oxygen evolution, as above

this potential water decomposition takes place instead of thickening of the oxide layer. In the case of Mg the electronic conductivity and, therefore, the resulting potential window for anodization depends on the electrolyte composition, since incorporation of electrolyte species in the growing oxide/hydroxide layers can produce layers showing greater blocking. A challenge to obtaining thick, compact layers on Mg by anodization is, however, achieving a low Pilling–Bedworth ratio for the formed oxide/hydroxide layers [73]. This leads to high internal stresses in the growing anodic films, and cracking of the layers can take place [74]. Adjustment of anodization parameters, such as the electrolyte concentrations, current density and anodization time, strongly affects the degree of porosity and quality of the oxide layer [75]. Similarly to chemical conversion, anodization is carried out in various baths, for example alkaline baths based on potassium hydroxide, and phosphate-, fluoride- or silicate-containing electrolytes. The bath composition is important not only to enable anodization at high voltages, as mentioned above, but also to reduce the dissolution of Mg during anodization. Within this technical field a range of patents exists on methods to produce such layers, e.g. Anomag, Magoxid and Anocast [76–78]. Patents related to this technology exist in the biomedical area, for example those of the company Biotronik [79]. Jo et al. [60] studied the effect of anodized layers on pure Mg on its corrosion behaviour in SBF. This was found to be minor compared with the effects of plasma electrolytic anodized surfaces (see below).

In addition to anodization approaches mainly used to thicken native oxide/hydroxide films on metal surfaces, dedicated anodization approaches have been explored to create nanoporous oxide layers. For Al and Ti alloys such approaches are well described in the literature. The key is to use an electrolyte leading to competition between anodic oxide growth and dissolution. Using the optimized electrochemical parameters self-organized growth of nanoporous or nanotubular oxide layers can be achieved [80–81]. However, for Mg alloys such approaches are still at a very early stage [82].

**2.1.4.2. Plasma electrolytic anodization.** Another route for formation of porous layers on Mg materials is anodization above the breakdown voltage, often called PEO, but also micro arc oxidation (MAO) or anodic spark deposition (ASD). As the very effective chromate coatings have been banned by EU regulation for automotive manufacturing [83] PEO has become the most commercially applied protection method for Mg alloys, e.g. Keronite coatings. The PEO equipment consists of an electrolytic bath, a working electrode consisting of the electrically connected Mg alloy component, and a stainless steel counter-electrode, which can be the wall of the cell in which the bath is contained. The quality and chemistry of the layer are determined by the bath and alloy properties and also by the processing parameters, such as the reaction time and potential. The applied voltages are higher than the dielectric breakdown potential of the growing oxide layer, usually up to 300 V [27,28], or even higher up to 400 [29] or 500 V [84]. During PEO discharges take place, a plasma is produced and an oxide layer grows. The process implies melting, flow of the melt, solidification, crystallization, partial sintering and densification of the growing oxide. As electrical discharges arise due to electric currents locally breaking through the growing layer, they produce characteristic craters on the surface. These pores typically have sizes of a few microns.

Anodized layers, especially those produced by plasma electrolytic oxidation, are more stable and inhibit corrosion better than chemical conversion layers [71]. Overall, PEO layers are very stable, hard and resistant to abrasion and corrosion. The disadvantages of PEO coatings are their brittleness and their electric isolation, which makes the method inappropriate for further processing via electric deposition. For orthopaedic implants such layers could be of inter-

est to slow down the corrosion rate as well as to act as a pre-treatment for organic based coatings. Hence, PEO layers should be used to protect the substrate in combination with a subsequent coating process and to promote coating adhesion.

**2.1.4.3. PEO oxide coatings.** Corrosion of PEO-treated Mg alloy samples in Hanks solution was first studied by Zhang et al. [85], then by Xu et al. [86] and, later, in SBF by Jo et al. [60]. In all studies PEO showed a lower corrosion current density in polarization studies than uncoated samples. Zhang et al. [85] additionally performed immersion and wear tests to demonstrate improved behaviour of the PEO-treated sample surfaces, which contains magnesium/aluminium oxide, magnesium silicate and magnesium/aluminium silicates. Xu et al. [86] used PEO as a pre-treatment to apply an organic based coating, however, no further analysis of the molten oxide particles on the PEO surface was carried out. Jo et al. [60] also used PEO as a pre-treatment, followed by immersion in SBF.

Gu et al. [29] demonstrated effects of voltage on the morphology of the PEO layer. Increasing the voltage led to an increase in layer thickness, as well as enlargement of the surface craters. As pores appeared due to dielectric breakdown, on greatly increasing the voltage the substrate surface became increasingly molten, and an eruption-like molten mass was deposited around the discharge channels in which gas bubbles were trapped. The author concluded that micropores are acceptable, however the gas bubbles and channels are not. This result was reflected in corrosion and cell culture studies. Tests were performed by immersion in Hanks solution, and the developing gas volume was measured. The corrosion resistance rose with anodization voltage up to 360 V. With higher voltages corrosion resistance decreased and more gas was evolved. In direct cell culture tests no MG63 cells survived after 5 days on uncoated samples, while the best performance after 5 days was by the PEO surface produced at 360 V in the special electrolyte used.

Gu et al. [29] compared the results of various immersion tests found in the literature, and PEO appeared the most effective method to reduce the corrosion rate, being even more effective than organic based coatings. An exception was a corrosion study of a PEO layer on a Mg–Zn–Ca alloy by Gao et al. [87], which showed no increase in corrosion resistance after the PEO treatment.

**2.1.4.4. PEO calcium phosphate coatings.** Using PEO it is also possible to produce calcium phosphate containing coatings [84,88]. In these studies the Ca/P ratio in the coating was controlled not only by adjustment of the reaction time and voltage but also by the addition of  $\text{Ca}^{2+}$  and phosphate to the electrolytic bath. Yao et al. [88] showed that control of the Ca/P ratio is possible, but they did not detect crystalline calcium phosphate phases in coatings having thicknesses up to 10  $\mu\text{m}$ . Srinivasan et al. [84] also produced coatings of various thicknesses, surface roughness and phase compositions, mostly without crystalline calcium phosphate. Only very high phosphate concentrations led to coatings containing dicalcium phosphate and calcium peroxide. The thickness also increased increasing  $\text{Na}_3\text{PO}_4$  concentration in the electrolyte bath.

**2.1.4.5. PEO fluoride coatings.** Shi et al. [89] applied fluoride-containing layers by PEO as a pre-treatment for the deposition of a sol–gel  $\text{TiO}_2$  coating on pure magnesium. The PEO layer had a thickness of about 12  $\mu\text{m}$ . SEM observations showed homogeneously distributed pores of a few microns in size on the surface. Whether the pores were permeable (open porosity) or not was not investigated. The corrosion resistance of the PEO layer was not studied, only that of the entire system being investigated, which is not discussed further in this review as the  $\text{TiO}_2$  sol–gel component is not biodegradable. A porous PEO fluoride coating was applied by Wu et al. [90] as a pre-treatment for electrophoretic

deposition (EPD) of calcium phosphate–chitosan coatings. In this approach porosity is necessary for the substrate to be electrically conductive during the EPD process [91].

### 2.1.5. Ion implantation

Studies have been also conducted considering ion implantation on magnesium alloys to improve corrosion resistance. Ion implantation leads to two or three layer structures with thicknesses of up to 1  $\mu\text{m}$  [92–94]. The implanted ions are able to form new oxides or compounds on the surface, which should affect the corrosion behaviour. Generally the improvements in corrosion resistance measured in Hanks solution or in NaCl solution were not significant, e.g. Al, Zr or Ti ions implanted in AZ91 [92], Ti ions implanted in AZ31 [95] or Ta ions in AZ31 [93]. However, Zn ions implanted in a Mg–Ca alloy [96] and N ions in AZ31 [95] decreased the corrosion resistance. Wu et al. [97] used the process of ion implantation as a pre-treatment to improve the adhesion between a titanium coating and a AZ31 substrate. Overall the process presents several disadvantages. Beside the cost, it is not appropriate for complex geometries of components such as implants and porous scaffolds.

## 2.2. Deposited coatings

### 2.2.1. General aspects

Deposited coatings can be divided into metal, inorganic and organic based coatings. The different application methods are shown in an overview in Fig. 2. The most relevant techniques applied, which reflect the state of the art in the literature, are comprehensively presented and discussed in this section.

**2.2.1.1. Metallic coatings.** The deposition of metals on magnesium is a technological challenge as magnesium shows high chemical reactivity and a low electrode potential. If the metallic coating is locally damaged galvanic corrosion will take place, leading to rapid degradation of the material. Additionally, several metals are not biocompatible in the sense of exhibiting controlled degradability and,

therefore, these non-degradable coatings are not considered in this review.

Of interest, however, is the coating of pure magnesium on a magnesium alloy substrate, which was studied by Fukumoto et al. [98]. The AZ31 alloy was coated with high purity magnesium by vapour deposition. Since adhesion between the deposition layer and substrate is poor, the process was supplemented by hot pressing and hot isostatic pressing (HIP). The results showed that the coating improved the corrosion resistance in salt solution. Furthermore, when the coating was locally broken the high purity magnesium coating worked as a sacrificial anode (cross-cut test).

**2.2.1.2. Inorganic coatings.** The deposition of inorganic coatings from the gas phase or other physical methods such as plasma spraying and laser application is inappropriate for geometrically complex components like implants and porous scaffolds. Moreover, physical deposition methods involve high energy consumption, high costs and complex facilities. Several authors have studied diamond-like carbon (DLC) coatings on Mg alloys [99,100], however, due to a lack of biodegradability of DLC, interest in DLC on magnesium alloys is limited. Therefore, in the following section only liquid-based methods for the deposition of inorganic coatings are considered, which correlate with wet chemical methods which are also suitable for organic based coatings (see Fig. 3). Liquid or wet chemical coating procedures are defined as techniques involving solutions, suspensions, colloids, or dissolved or suspended precursors [101].

**2.2.1.3. Organic coatings.** Organic based coatings are attractive for biomedical applications as they offer protection against corrosion and other functions, such as drug delivery and an ability to be functionalized with organic biomolecules. The method most applied to obtain organic coatings is simple dipping in an organic based solution (see Fig. 3). Composite systems can be developed by the use of inorganic pre-treatments. The thickness of organic based coatings

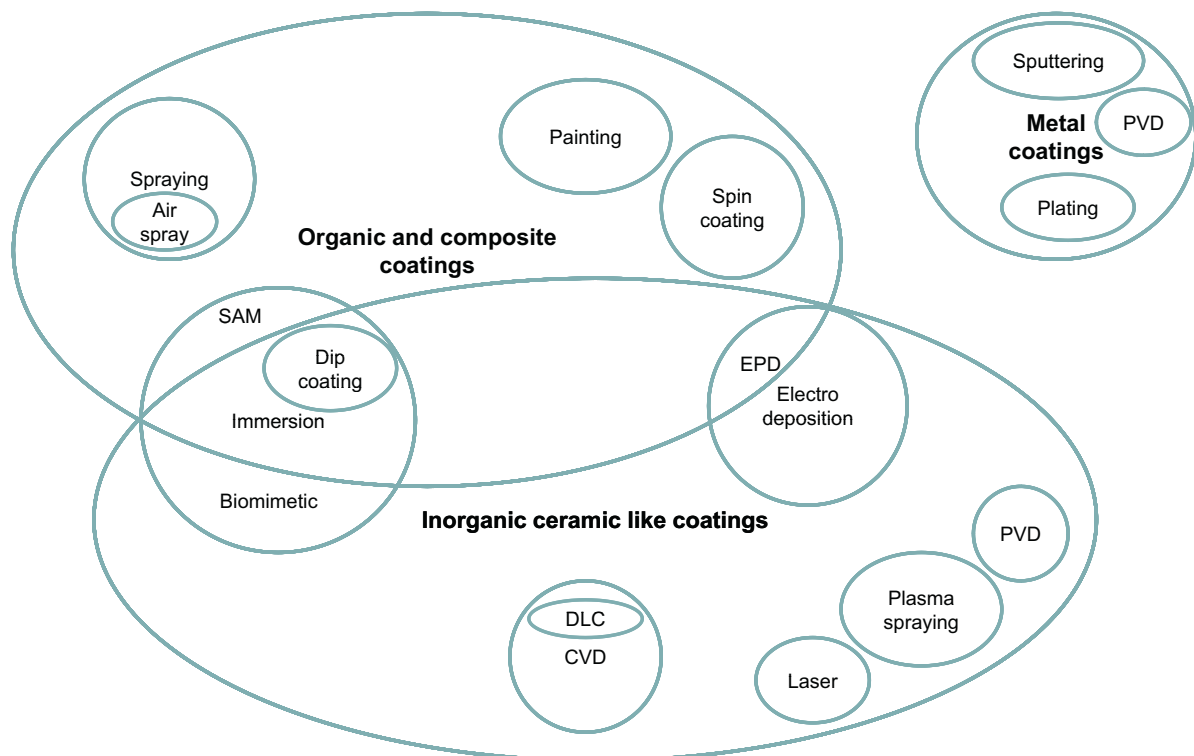
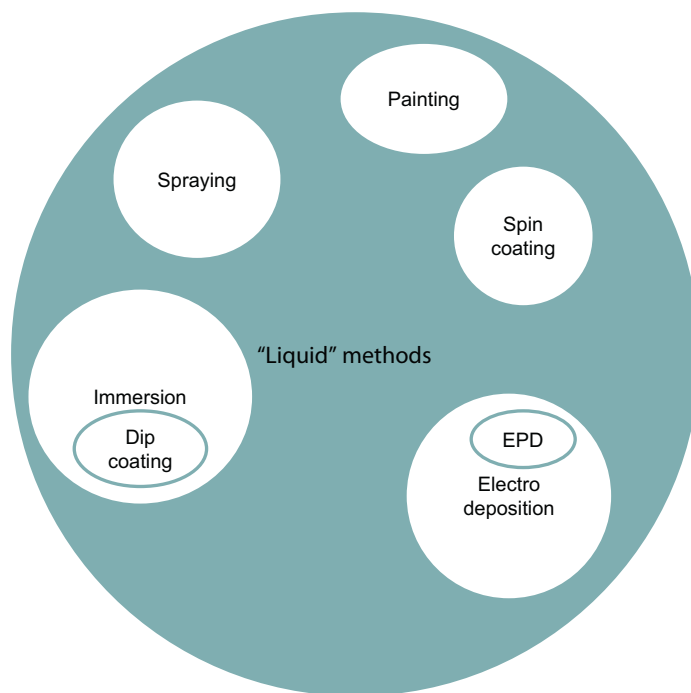


Fig. 2. Schematic diagram showing the range of technologies suitable for deposited coatings.



**Fig. 3.** Overview of liquid or wet chemical coating procedures, which are defined as production methods including solutions and suspensions to produce inorganic or organic based coatings.

may vary from several nanometres in the case of self-assembled monolayers up to several hundred microns.

A large number of patents on organic based biomedical coatings on magnesium alloys exist [102–105]. However, particular deposition methods are not described in detail, the content of the patents is focussing mostly on the developed compositions.

### 2.2.2. Cathodic electrodeposition

This method mainly concerns the deposition of inorganic phases. The relevant literature reveals that cathodic electrodeposition leads to better results in the production of HA layers than chemical conversion layers. However, careful adjustment of the parameters is necessary. Sometimes there are traces of the substrate mixed into the coating forming new phases, such that the coating is not purely by deposition but also to some extent by conversion at the interface.

Song et al. [106] produced HA layers on Mg alloy AZ91 in a two-step process. First dicalcium phosphate dihydrate (DCPD) and  $\beta$ -tricalcium phosphate ( $\beta$ -TCP) were formed by electrodeposition (ED). Subsequently the specimens were immersed into NaOH solution to develop a HA coating. This coating system was shown by electrochemical polarization and impedance studies to slow down the corrosion process in SBF. The formation of DCPD by ED and subsequent transformation into HA was repeated in other studies, discussed further below.

Wen et al. [107] also applied a two step process to the Mg alloy AZ31 which involved slightly changing the electrolyte composition, the reaction times and temperatures, thereby producing fine microstructures. After the second step the structure changed from platelets to nanowhiskers. The HA produced was analysed and exhibited doping with several other ions. The investigation also included corrosion polarization studies in SBF which demonstrated increased corrosion resistance after coating. Kannan and Orr [108] applied a three step process to Mg alloy AZ91 by incorporating an additional immersion in NaOH solution before electrodeposition. HA coatings were produced having a microstructure formed of rod-shaped particles. The study included mechanical tensile

testing, which showed that the coating improved the in vitro mechanical strength by 20% (all test samples were exposed to SBF prior to testing). It was also found that applying very high voltages during electrodeposition produced coatings without protective properties.

Wu et al. [90] also applied a three step process to AZ91D alloy substrates by adding an immersion treatment in phosphate-buffered saline (PBS) for up to 15 days after PEO and a final EPD treatment to develop an organic–inorganic composite coating. The EPD process was performed using six different mixtures of HA/chitosan as the electrolytes. The study focused on the mechanism of formation of a composite coating made of calcium phosphate–chitosan, adjusting the proportions of HA, DCPD and  $\text{Ca}(\text{OH})_2$  in the coating. Thereby EPD produced nanoscale HA and  $\text{Ca}(\text{OH})_2$  layers, with the subsequent buffer treatment possibly converting  $\text{Ca}(\text{OH})_2$  to HA and DCPD. However, the buffer treatment did not convert all Ca phases into HA, even after 15 days immersion. The adhesion of the coatings was seen to depend on the composition of the bath suspension.

### 2.2.3. Sol–gel coatings

Producing inorganic biodegradable coatings on magnesium alloys by dip coating without reactions with the substrate is uncommon. There have been studies of sol–gel based coatings including subsequent heat treatment steps, required to densify the ceramic layer and improve the corrosion resistance. However, only non-degradable coatings were produced. For example, Feil et al. [109] produced  $\text{SiO}_2$  layers from sols via dipping and also via EPD on Mg alloy AZ31. Shi et al. [89] showed the feasibility of this technique on pure magnesium using a  $\text{TiO}_2$  sol. The coating process had to be repeated several times to obtain a coating thick enough to cover the pores in the pre-treated PEO layer and the  $\text{TiO}_2$  phase remained amorphous. Zhong et al. [110] applied  $\text{Al}_2\text{O}_3$  sols and deposited the coatings by spin coating. Spin coating is a technique for the application of a coating onto a flat surface and thus is inappropriate for complex shaped or porous implants and scaffolds. Lalk et al. [111] reported an in vivo study on degradable magnesium

sponges coated with a bioactive glass, however, it is not clear from the original publication how the sol–gel coating was produced. Another coating based on a bioactive glass was produced by Seitz et al. [69]. However, it was made by dispersing milled glass powder and not using the sol–gel route (see Section 2.2.4). Roy et al. [112] synthesized thick porous calcium phosphate and Si-containing calcium phosphate coatings via a sol–gel method. The Si-containing layers showed higher concentrations of HA. These films were tested for degradation by immersion in Dulbecco's modified Eagle's medium and were stable for at least 3 days. Overall the films were inadequate to reduce degradation of the substrate due to the existing porosity and the presence of cracks. MC3T3-E1 cell tests showed that the coated substrates were more cytocompatible than uncoated substrates.

#### 2.2.4. Dipping and immersion

Dip coating to obtain organic biopolymer coatings on Mg and Mg alloy substrates has received wider attention than dip coating of inorganic coatings.

**2.2.4.1. Organic coating in one step.** Li et al. [113], for example, produced a polylactic-co-glycolic acid (PLGA) coating on Mg6Zn substrates. The coating thickness (33 and 72  $\mu\text{m}$ ) was determined by the PLGA concentration. Corrosion tests using polarization and impedance techniques performed in NaCl solution demonstrated a reduced degradation rate due to the presence of the biopolymer coating. The thick (72  $\mu\text{m}$ ) coating showed lower corrosion resistance than the thin (33  $\mu\text{m}$ ) coating, probably due to its poorer quality, e.g. voids and flaws. Direct cell culture tests with mouse osteoblast-like MC3T3-E1 cells on the thin coatings revealed enhanced cell attachment due to the PLGA coating.

Chen et al. [114] successfully prepared polycaprolactone (PCL) and polylactic acid (PLA) coatings with thicknesses of about 15–20  $\mu\text{m}$  on the surface of pure magnesium. Conventional static polarization tests and dynamic immersion corrosion tests were performed in SBF to simulate stent conditions. Besides some improvement in corrosion resistance caused by the presence of the coatings, dynamic degradation tests indicated a specific interaction between the substrate and polymer coating which undermined the corrosion resistance. This study suggested that this interaction may also occur for implanted magnesium stents coated with biodegradable polymers, which could be a major challenge for the further development of drug-eluting magnesium stents.

**2.2.4.2. Organic based coating in two steps.** Xu et al. [86] presented a two step coating process for alloy WE42, involving a preliminary PEO treatment followed by dropping the organic phase onto the surface. The organic phase was a cross-linked gelatin/PLGA particle solution, in which 150–300 nm sized particles were loaded with paclitaxel to realize a drug release system. Corrosion studies using polarization and EIS methods in Hanks solution showed increased corrosion resistance after coating, however, there was little difference in corrosion resistance after the PEO treatment and after the entire two step process. The main tasks of the composite coating were to control drug release and to control corrosion of the PEO surface.

Gao et al. [87] also developed a coating process including preliminary PEO treatment of a substrate followed by immersion in an organic phase. The PEO-treated Mg–Zn–Ca alloy was immersed in a solution of propolis, ethanol and PLA. The process is time consuming, as the samples must be immersed several times and dried. The corrosion resistance in SBF was improved by the composite coating. Furthermore, the coating promoted cell adhesion and proliferation using Whartons jelly derived mesenchymal stem cells.

In a related study Ng et al. [39] presented a two step process, involving preliminary hydrothermal treatment to produce a layer

of  $\text{Mg}(\text{OH})_2$ , then immersion in stearic acid for 2 h at various temperatures and stearic acid concentrations. As the magnesium hydroxide showed a platelet-like morphology and a layer thickness of 170  $\mu\text{m}$  adjustment of the viscosity of the organic phase was important to facilitate penetration of the stearic acid. Finally, a composite coating was achieved composed of (i)  $\text{Mg}(\text{OH})_2$  anchoring the subsequent organic coating, (ii) magnesium stearate placed between  $\text{Mg}(\text{OH})_2$  and stearic acid and (iii) a stearic acid layer on the outer surface. As a reaction took place with the substrate the composite coating could be partially characterized as being a type of conversion coating. Overall, the focus of the study was an extensive analysis of the coating. Polarization tests and EIS combined with immersion tests for up to 80 days in Hanks solution revealed that the composite coatings increased the corrosion resistance of the substrate. Along with degradation of the coating, apatite phases were seen to form on the surface. The adhesion properties of the coating were also evaluated using a tape test and the high adhesiveness attributed to physical interlocking of the plate-like structure of the  $\text{Mg}(\text{OH})_2$  layer and to the bond enhancing formation of magnesium stearate.

Dip coating with chitosan was found to improve the corrosion resistance of a Mg–Ca alloy immersed in SBF [115], with the quality of the coating depending on the molecular weight of the chitosan and the number of coating cycles. Silanization of the substrates was performed as a pre-treatment, but the adhesion of the coating was not discussed.

**2.2.4.3. Inorganic coating.** Seitz et al. [69] dispersed bioactive glass particles in ethanol and dip coated Mg–Nd alloy samples. The dip coated substrates were heat treated at 500  $^\circ\text{C}$  for 168 h and an amorphous layer 10  $\mu\text{m}$  thick formed. The corrosion tests in a dynamic SBF environment showed no increase in corrosion resistance, and even a slight decrease. The reason for that remains open, although factors such as a possible decrease in pH caused by ion exchange between the coating and medium or eventual microcracking of the coating could have accelerated the corrosion process.

#### 2.2.5. Spraying

Wong et al. [116] developed an air spray technique using PCL in dichloromethane (DCM) solution. The coating had to be applied layer by layer, with the flow and temperature being adjustable. In this way control of the thickness and homogeneity of the porous polymer-based membrane was possible. The resulting thickness range, however, was not mentioned in the study. Using alloy AZ91 samples as substrates two different concentrations of PCL were applied to produce low and high porosity membranes with pore sizes of up to 3.2  $\mu\text{m}$ . Polarization and immersion tests in SBF were carried out, which showed that the polymer coating reduced the degradation rate, which was controlled by the degree of porosity. The polarization curves, however, showed that the corrosion current density was about one order of magnitude lower, which was the same degree of decrease as that found by Chen et al. [114], who also applied a thin PCL layer, whereas a thicker layer of PLGA [113] and other organic based systems combined with pre-treatments [39,86,87] decreased the corrosion current by about two or three orders of magnitude. In vitro tests using SaOS-2 human osteoblasts showed improved cytocompatibility of the polymer-coated samples, and in vivo tests demonstrated the formation of a relatively high volume of new bone. After 2 months implantation no inflammation and no gas accumulation were found for both coated and uncoated samples.

Hahn et al. [117] used aerosol deposition on AZ31 alloy samples, sprayed in vacuo with a specially mixed HA–chitosan powder at room temperature. The nozzle was placed vertically opposite the sample, which allows rotation in the x- and y-directions but not in

the z-direction. After coating the corrosion behaviour of the samples was tested in SBF. Polarization curves showed an improvement in corrosion resistance after deposition for all applied HA-chitosan coatings, but increasing addition of chitosan appeared to lower the corrosion resistance. Adhesion tensile strength tests revealed good adhesion (about 25 MPa), which is impressive when related to the fact that no special pre-treatment of the substrates was performed.

### 3. Discussion

Critical factors for the application and use of biodegradable coatings on Mg and Mg alloys for biomedical applications are given below.

#### 3.1. Surface chemistry

Specific surface chemistry requirements depend on the targeted application, e.g. stents, orthopaedic implants, or tissue engineering scaffolds. Reviewing the literature, the greatest interest has been for calcium phosphate-containing (see Table 1) and organic based (see Table 2) coatings. There are also patents for calcium phosphate-containing coatings on medical implants [118]. However,

in spite of the large number of studies to date, the results in the literature demonstrate difficulties in adjusting the required phases in the coatings.

Chen et al. [56] concluded in a review of chemical conversion coatings on Mg and its alloys that the coating pre-treatment appears to be more significant than the choice of coating technology itself. Our analysis of the literature suggests that this can be applied to organic based coatings as well. Pre-treatment is necessary to functionalize the surface and to control the coating processes, especially in aqueous solutions, as dissolution during the coating process can be a strong side-reaction.

#### 3.2. Corrosion rate

Corrosion studies were carried out in about 75% of the reviewed papers. The specific test methods most commonly used were immersion tests, polarization studies and impedance spectroscopy. The composition, concentration and volume of the electrolyte, as well as the test time and other parameters, were varied. Due to this variation in experimental conditions comparison of the results is very difficult. Overall all coatings were found to reduce the corrosion rate to a certain extent, as expected.

Gu et al. [29], comparing the results of immersion tests in the literature, concluded that PEO on Mg and Mg alloys appeared to

**Table 1**  
Calcium phosphate coating by different methods.

Refs.	Substrate	Thick-ness	Method	Layer	$i_{\text{corr}}$	in vitro	in vivo
<b>Chemical conversion</b>							
[37]	Mg	Tens of $\mu\text{m}$	Immersion in m-SBF at 37° for 5 days	Amorphous Ca/Mg-phosphate		X	
[57]	WE43	>20 $\mu\text{m}$	Immersion in m-SBF at 37° for 5 days	Amorphous carbonated Ca/Mg-phosphate			
[60]	Mg		Immersion in SBF for 7 days after various anodization treatments	Ca and P		X	
[65]	AZ31		Immersion in $\text{Na}_2\text{HPO}_4 \cdot 12\text{H}_2\text{O}$ , $\text{NaHCO}_3$ , $\text{Ca}(\text{NO}_3)_2 \cdot 4\text{H}_2\text{O}$ at 37 °C for 24 h	Amorphous Ca/Mg-phosphate			X
[61]	Mg, AZ31, AZ61	3–4.0 $\mu\text{m}$	Immersion in Ca-EDTA + $\text{KH}_2\text{PO}_4$ , NaOH solution at 95 °C for 8–24 h, pH variation	HA, $\text{Mg}(\text{OH})_2$ , sometimes $\beta$ -TCP			
[62]	AZ31	10 nm < x < 3 $\mu\text{m}$	3-step: immersion in NaOH solution at RT for 24 h, then 140 °C for 24 h, then immersion in $\text{CaCl}_2$ + $\text{Na}_2\text{HPO}_4$ solution at pH = 5	Poorly crystalline Ca / Mg - HA			
[63]	Mg	200–300 nm	2-step: immersion in $\text{Ca}(\text{NO}_3)_2 \cdot 4\text{H}_2\text{O}$ + $\text{Na}_3\text{PO}_4$ + $\text{HNO}_3$ solution at 65 °C for 2 min, then NaOH solution at 80 °C for 60 min	Ca-deficient HA / $\text{Mg}(\text{OH})_2$	X		
[64]	Mg-1.2Mn-1.0Zn		3-step: immersion in alkaline solution at 63 °C for 15 min, then immersion in $\text{H}_3\text{PO}_4$ + $\text{H}_2\text{SO}_4$ solution at RT for 5–10s, then immersion in $\text{H}_3\text{PO}_4$ + $\text{Ca}(\text{H}_2\text{PO}_4)_2 \cdot 2\text{H}_2\text{O}$ + $\text{Zn}(\text{H}_2\text{PO}_4)_2 \cdot 2\text{H}_2\text{O}$ + $\text{NaNO}_3$ + $\text{NaNO}_2$ solution for 6 min	Mainly brushite $\text{CaHPO}_4 \cdot 2\text{H}_2\text{O}$ and some $\text{Mg}^{2+}$ and $\text{Zn}^{2+}$		X	X
<b>Anodization</b>							
[88]	AZ91D	3–5 $\mu\text{m}$	PEO in NaOH + $(\text{NaPO}_3)_6$ + $\text{Ca}(\text{H}_2\text{PO}_2)_2$ solution	Mg, Al, P and Ca, and little crystallized MgO	X		
[88]	AZ91D	8–10 $\mu\text{m}$	PEO in $\text{Na}_2\text{SiO}_3$ + $(\text{NaPO}_3)_6$ + $\text{Ca}(\text{H}_2\text{PO}_2)_2$ solution	Mg, Al, Si, P and Ca, crystallized $\text{Mg}_2\text{SiO}_4$ and MgO	X		
[84]	AM50	in the range of 20–70 $\mu\text{m}$	PEO in $\text{CaOH}_2$ + $\text{Na}_3\text{PO}_4$ solution in different mass ratios	MgO, $\text{Mg}_3(\text{PO}_4)_2$ , amorphous Ca-phases, $\text{CaH}(\text{PO}_4)_2$ , $\text{CaO}_2$	X		
<b>Electrodeposition</b>							
[106]	AZ91		2-step: ED in $\text{Ca}(\text{NO}_3)_2$ + $\text{NH}_4\text{H}_2\text{PO}_4$ + $\text{H}_2\text{O}_2$ solution at 4 V at RT for 2 h, then immersion in NaOH solution at 80 °C for 2 h	ED: DCPD and $\beta$ -TCP, post-treatment: HA	X		
[107]	AZ31	10 $\mu\text{m}$	2-step: ED in $\text{Ca}(\text{NO}_3)_2$ + $\text{NH}_4\text{H}_2\text{PO}_4$ + $\text{NaNO}_3$ solution at 85 °C for 1 h, then immersion in NaOH solution at 80 °C for 4 h	ED: DCPD, post-treatment: HA, detected: Ca, P, O, Na, Mg and C	X		
[108]	AZ91	about 10–20 $\mu\text{m}$	3-step: immersion in NaOH solution at 80 °C for 1 h, then ED in $\text{Ca}(\text{NO}_3)_2$ + $\text{NH}_4\text{H}_2\text{PO}_4$ solution, then immersion in NaOH solution at 80 °C for 1 h	ED: DCPD, post-treatment: HA			
<b>Sol gel</b>							
[112]	Mg4Y	50 $\mu\text{m}$	synthesis using calcium nitrate and phosphorus pentoxide, for Si containing layers additional tetraethyl orthosilicate, heat treatment at 450 °C for 24 h	$\beta$ -TCP and HA		X	

$i_{\text{corr}}$ , corrosion current density determined by corrosion tests via polarization.

**Table 2**

Organic based coating by different methods.

Refs.	Substrate	Thickness	Method	Layer	$i_{\text{corr}}$	in vitro	in vivo
[113]	Mg6Zn	33 $\mu\text{m}$ and 72 $\mu\text{m}$	Dipcoating in PLGA-chloroform solution	PLGA	X	X	
[114] [86]	Mg WE42	About 10 $\mu\text{m}$	Dip coating in PCL or in PLA solution at RT 2-step: PEO, then gelatin / PLGA nanoparticles solution was dropped onto the surface, then dried at RT	PCL or PLA cross-linked gelatin / PLGA nano-sphere composite	X X		
[87]	Mg-Zn-Ca		Several-step: PEO, then immersion and 3 times dipping into propolis + ethanol + PLA	detected: C, O, Cl, P, Na, Ca	X	X	
[39]	Mg	In the range of 180–230 $\mu\text{m}$	2-step: hydrothermal treatment, then immersion into stearic acid for 2 h, various concentrations and temperatures	Mg(OH) <sub>2</sub> , stearic acid, Mg-stearate	X		
[90]	AZ91D		3-step: PEO pre-treatment, EPD in 6 different solutions (0–100vol% HA/chitosan additions), then immersion in PBS at 37 °C for 15 days	HA-DCPD, chitosan, Ca(OH) <sub>2</sub>			
[116]	AZ91		Several-step: spraying application of 2 different concentrations of PCL in DCM solution, layer-by-layer	Low and high porosity membrane	X	X	X
[117]	AZ31	5 $\mu\text{m}$	Spraying various HA-chitosan compositions	HA-chitosan composite, example: 10% chitosan	X	X	

 $i_{\text{corr}}$ , corrosion current density determined by corrosion tests via polarization.**Table 3**

Polarization measurements on several coated Mg substrates tested under different conditions, as reported in the literature.

Refs.	Conditions	Substrate	$i_{\text{corr}}$	$E_{\text{corr}}$	Coating method	$i_{\text{corr}}$	$E_{\text{corr}}$
[39]	Hanks solution 37 °C	AZ31	$2.51 \times 10^{-5}$ A/cm <sup>2</sup>	−1.6 V (SCE)	Hydrothermal oxide/hydroxide	$4 \times 10^{-6}$ A/cm <sup>2</sup>	−1.71 V(SCE)
[67]	Hanks solution 37 °C	Mg	400 $\mu\text{A}/\text{cm}^2$	−1.85 V (SCE)	Chemical conversion fluoride	10 $\mu\text{A}/\text{cm}^2$	−1.58 V(SCE)
[63]	MEM, 37 °C	Mg	$6 \times 10^{-4}$ A/cm <sup>2</sup>		Chemical conversion Ca-phosphate	$2.7 \times 10^{-6}$ A/cm <sup>2</sup>	
[60]	SBF 37 °C	Mg	380 $\mu\text{A}/\text{cm}^2$	−1.97 V (SCE)	PEO	161 $\mu\text{A}/\text{cm}^2$	−1.97 V (SCE)
[85]	Hanks solution 37,5 °C	AZ91	0.028703 A/cm <sup>2</sup>	−1.5786 V	PEO	$2.0456 \times 10^{-7}$ A/cm <sup>2</sup>	−0.43019 V
[88]	0.9% NaCl	AZ91D	$2.256 \times 10^{-5}$ A (1cm <sup>2</sup> )		PEO Ca-phosphate various compositions	$5.478 \times 10^{-7}$ and $6.339 \times 10^{-7}$ A (1cm <sup>2</sup> )	
[84]	0.1 M NaCl 20±2 °C	AM50	$1.8 \times 10^{-2}$ mA/cm <sup>2</sup>	−1452 mV (Ag/AgCl)	PEO Ca-phosphate in different mass ratios	Range: $3.5\text{--}23.0 \times 10^{-5}$ mA/cm <sup>2</sup>	About −1500 mV (Ag/AgCl)
[106]	SBF, 37 °C	AZ91	$2.97 \cdot 10^{-4}$ A/cm <sup>2</sup>		Electrodeposition Ca-phosphate	$3.65 \times 10^{-5}$ A/cm <sup>2</sup>	Decrease
[107]	Hanks solution, 37 °C	AZ31	$2.51 \times 10^{-5}$ A (1cm <sup>2</sup> )	−1.6 V	Electrodeposition Ca-phosphate	$3.98 \times 10^{-8}$ A (1cm <sup>2</sup> )	−1.42 V
[113]	0.9% NaCl 37 °C	Mg6Zn	$26.5 \times 10^{-6}$ A/cm <sup>2</sup>	−1.46 V	Dipcoating PLGA various concentrations	$0.085 \times 10^{-6}$ and $0.097 \times 10^{-6}$ A/cm <sup>2</sup>	−1.44 V and −1.36 V respective
[114]	SBF + Hepes 37 °C	Mg	$2.073 \times 10^{-4}$ A (1cm <sup>2</sup> )		Dipcoating PCL	$1.293 \times 10^{-5}$ A (1cm <sup>2</sup> )	Increase $\Delta E = 246.4$ mV
[114]	SBF + Hepes 37 °C	Mg	$2.073 \times 10^{-4}$ A (1cm <sup>2</sup> )		Dipcoating PLA	$3.565 \times 10^{-5}$ A (1cm <sup>2</sup> )	Increase $\Delta E = 120.1$ mV
[86]	Hanks solution, 37 °C	WE42			PEO and infiltration gelatin/PLGA	Decrease	Increase
[87]	SBF, 36.5 ± 0.5 °C	Mg-Zn-Ca	$3.36 \times 10^{-4}$ A/cm <sup>2</sup>		PEO and infiltration propolis	$1.10 \cdot 10^{-6}$ A/cm <sup>2</sup>	Decrease $\Delta E = 240$ mV
[39]	Hanks solution, 37 °C	Mg	$0.25 \times 10^{-3}$ A/cm <sup>2</sup>	−1.80 V	Infiltration stearic acid, various thicknesses	$0.12 \times 10^{-6}$ , $0.14 \times 10^{-6}$ and $11.2 \times 10^{-9}$ A/cm <sup>2</sup>	−1.49, −1.46 and −1.45 V(SCE) respective
[116]	SBF, 37 ± 0.5 °C	AZ91			Spraying PCL low and high porosity membrane	Decreased	Increase $\Delta E = 1444$ mV and 1114 mV
[117]	SBF, 37 °C	AZ31	$3.893 \times 10^{-4}$ A/cm <sup>2</sup>	−1.733 V	Spraying HA-chitosan, example 10% chitosan	$3.144 \times 10^{-5}$ A/cm <sup>2</sup>	−1.581 V
[95]	3.5% NaCl	AZ31	$4.948 \times 10^{-5}$ A/cm <sup>2</sup>	−1.455 V	N ion implantation	$2.058 \times 10^{-5}$ A/cm <sup>2</sup>	−1.450 V

 $i_{\text{corr}}$ , corrosion current density;  $E_{\text{corr}}$ , corrosion potential.

produce coatings which were more effective than others. Gu et al. [29] found that PEO resulted in a more than 90% reduction in corrosion rate, whereas other coatings, e.g. alkaline and fluoride treated surfaces and organic based coatings, produced between about an 50% and 80% reduction. However, even PEO coatings did not show a 100% reduction in corrosion rate. Indeed, the key function of coatings on Mg for biodegradable applications is to cause a temporary inhibition but not complete suppress corrosion of the material in a physiological environment.

The most commonly used means to determine corrosion rates of the coatings was the potentiodynamic polarization method (see Table 3). This electrochemical technique was performed in SBF or NaCl solution, and corrosion protection in the presence of the coatings was determined on the basis of the corrosion current density  $i_{\text{corr}}$ . The reduction in  $i_{\text{corr}}$  for both types of coatings using SBF as the corrosion test electrolyte was in the range 1–3 orders of magnitude [39,63,86,87,106,107,114,116,117]. These data suggest that the corrosion rate is adjustable. However, there is concern

regarding the uniformity and long-term nature of the corrosion process. Information on these issues cannot be revealed by carrying out polarization measurements alone.

### 3.3. Long-term corrosion behaviour

Generally *in vitro* and *in vivo* tests have indicated that most of the coatings developed can delay the start of corrosion. In spite of coating for the lifetime of the medical device, the right alloy choice is also important as the coating will disappear with time. It has been reported that the accumulation of subcutaneous gas bubbles depends on the phases and microstructure of the magnesium alloy used and on the geometry of the samples rather than on the coating itself [68,116].

Another important issue is the degradation process over the long term. In this context it should be pointed out that many reports in the literature only studied the *in vitro* corrosion behaviour over a period of a maximum of a few days, which does not provide sufficient information to extrapolate for the whole lifetime of the implants. Li et al. [113] adapted the degradation model of Hänzli et al. [35] for PLGA coatings and proposed a sigmoidal corrosion law over time for the coated surface, compared with a parabolic law for the uncoated surface (see Fig. 4). A greater amount of data on the long-term corrosion behaviour and on *in vitro* and *in vivo* studies will need to be evaluated to understand how to control the degradation of coated samples. For that, the impact of coating adhesion, thickness and topography has to be considered in more detail.

### 3.4. Uniformity of the corrosion process

An issue which is often neglected when reporting on the corrosion behaviour of coated Mg alloys is the influence of the coating on the dissolution morphology. For non-coated Mg alloys, as previously mentioned, typically highly non-uniform dissolution takes place over the surface. For coated samples corrosion may start at certain defects present in the coating, and therefore also be non-uniform in nature. After corrosion initiation at defects, fracture and flaking off of the coating could take place by dissolution propagation (e.g. by filiform corrosion). Such defects were found to be present in many calcium phosphate-containing coatings, in the

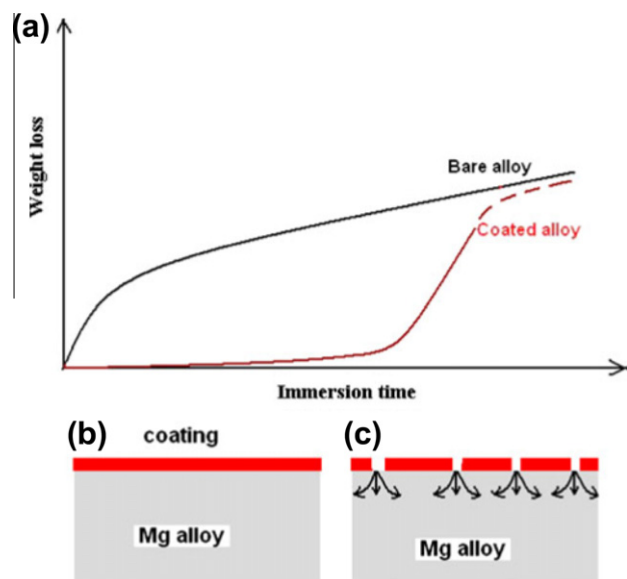


Fig. 4. Degradation model for PLGA coatings according to Li et al. [113], with permission from Springer.

form of cracks and pores. In organic based coatings there is a risk of corrosion taking place between the coating and substrate, which may lead to detachment of the coating. Pre-treatments for organic coatings can help to prevent such deleterious corrosion processes of coated samples. Therefore, even though development of the “perfect” barrier coating for biodegradable Mg alloys may not be required, the coatings should provide sufficient corrosion protection for the given application, and they should lead to a well-defined degradation rate and dissolution behaviour.

### 3.5. Adhesion

It is remarkable that no studies on calcium phosphate-containing layers, listed in Table 1, included adhesion tests. Even if there are processes proposed consisting of more than one step, the pre- and post-treatments are not considered as promoting adhesion. Those treatments were performed primarily to adjust the calcium phosphate phases, often with the aim of developing HA layers. However, some SEM studies have shown the presence of cracks. Cracking can develop during coating due to corrosion taking place, and in other cases during dehydration during the drying process. One example is presented in Fig. 5. Cracks are an indication of low adhesion and may lead to sigmoidal degradation behaviour of the coating. Roy et al. [112] studied the degradation behaviour of calcium phosphate films, showing that the layers were only stable for 3 days and did not provide sufficient protection against degradation due to the presence of pores and cracks.

For organic based coatings pre-treatments are often performed to create a bond between layers (see Table 2). Often the bonding is merely physical interlocking of the phases. However, adhesion tests for polymer or composite coatings have rarely been performed.

### 3.6. Coating morphology

The thickness of calcium phosphate based coatings ranges over three orders of magnitude (from 0.2 to 200  $\mu\text{m}$ ). The thicknesses of organic based coatings are theoretically from several nanometres up to hundreds of microns. Indeed, the appropriate thickness for each application has to be carefully selected.

The surface topography will have a significant impact on the corrosion behaviour, as well as on cell adhesion. Most of the studies discussed in this review used SEM to observe the surface. However, there is still a lack of information on the correlation between surface roughness, surface morphology, corrosion behaviour and cytotoxicity. Nanostructuring and functionalisation using proteins to enhance cell response [81,119], as is known for other materials, represent an attractive subject for future research to improve the biocompatibility of coatings on Mg and Mg alloys.

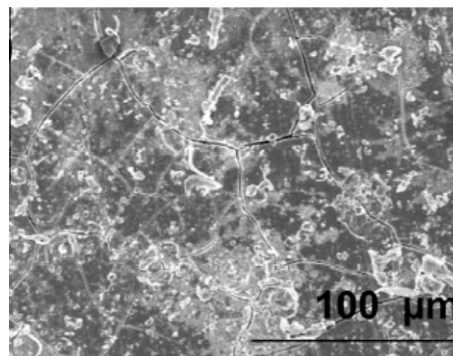


Fig. 5. SEM images of the surface of Mg samples soaked in m-SBF at 37 °C for 5 days, according to Lorenz et al. [37], with permission from Elsevier.

Furthermore, specific requirements of the surface modification approaches depend on the targeted application, e.g. stents, orthopaedic implants, or tissue engineering scaffolds. For example, the mostly porous and rough surfaces after anodization are not appropriate for stents.

#### 4. Conclusions

This analysis of the literature has revealed that a wide range of coatings on Mg and Mg alloys can increase the corrosion resistance of these materials. Appropriate test methods (like EIS) have to be further developed to obtain accurate information on the uniformity of the corrosion behaviour during long-term exposure. Functionalities achieved by the coatings, besides increasing the corrosion resistance of the substrates, are controllable degradability and improved osseointegration, as demonstrated by in vitro and in vivo testing. In addition, organic based coatings have shown the capability to act as local drug delivery platforms, however, only a few studies have focused on this topic, indicating that the development of these coatings is in its infancy. Calcium phosphate-containing coatings are very common, but in many cases satisfactory results were not achieved, typically due to crack formation or badly controlled adjustment of the specific calcium phosphate phases. As a concluding remark it can be stated that most studies to date have concentrated on one or two coating properties and the whole range of functionalities and coating properties have not been explored simultaneously. However, complete characterization is important for use as implants, including all critical factors such as corrosion rate, surface chemistry, adhesion, and coating morphology.

#### Appendix A. Figures with essential colour discrimination

Certain figures in this article, particularly Figs. 1–4, are difficult to interpret in black and white. The full colour images can be found in the on-line version, at <http://dx.doi.org/10.1016/j.actbio.2012.04.012>.

#### References

- [1] Cho K et al. Magnesium technology and manufacturing for ultra lightweight armored ground vehicles, ARL-RP-236. Aberdeen Proving Ground, MD: Army Research Laboratory; 2009.
- [2] Eliezer D, Aghion E, Froes FH. Magnesium science, technology and applications. *Adv Perform Mater* 1998;5:201–12.
- [3] James DW. Review paper. High damping metals for engineering applications. *Mater Sci Eng* 1969;4(1):1–8.
- [4] Lin B, Kuo C. Application of an integrated RE/RP/CAD/CAE/ CAM system for magnesium alloy shell of mobile phone. *J Mater Process Technol* 2009;209:2818–30.
- [5] Gray JE, Luan B. Protective coatings on magnesium and its alloys – a critical review. *J Alloys Compd* 2002;336:88–113.
- [6] Guo KW. A review of magnesium/magnesium alloys corrosion and its protection. *Recent Patents Corros Sci* 2010;2:13–21.
- [7] Staiger MP, Pietak AM, Huadmai J, Dias G. Magnesium and its alloys as orthopedic biomaterials: a review. *Biomaterials* 2006;27:1728–34.
- [8] Zeng R, Dietzel W, Witte F, Hort N, Blawert C. Progress and challenge for magnesium alloys as biomaterials. *Adv Eng Mater* 2008;10:B3–B14 [+702].
- [9] Witte F et al. Degradable biomaterials based on magnesium corrosion. *Curr Opin Solid State Mater Sci* 2008;12:63–72.
- [10] Witte F. The history of biodegradable magnesium implants: a review. *Acta Biomater* 2010;6:1680–92.
- [11] Bayer U, Schmidt J, Leitel A. Plasmachemische Oxidation von Magnesiumlegierungen – Anwendungen in optischen Geräten und Fahrzeugbau. *Galvanotechnik* 2003;9:2161–8.
- [12] Rodrigues LR. Inhibition of bacterial adhesion on medical devices. *Adv Exp Med Biol* 2011;715:351–67.
- [13] Bellucci D, Cannillo V, Cattini A, Sola A. A new generation of scaffolds for bone tissue engineering. *Ind Ceram* 2011;31(1):59–62.
- [14] Boccaccini AR, Blaker JJ. Bioactive composite materials for tissue engineering scaffolds. *Expert Rev Med Devices* 2005;2(3):303–17.
- [15] Mourino V, Boccaccini AR. Bone tissue engineering therapeutics: controlled drug delivery in three-dimensional scaffolds. *J R Soc Interface* 2010;7(43):209–27.
- [16] Song G, Atrens A, Wu X, Zhang B. Corrosion behavior of AZ21, AZ501 and AZ91 in sodium chloride. *Corros Sci* 1998;40(10):1769–91.
- [17] Hoog OC, Birbilis N, Zhang MZ, Estrin Y. Surface grain size effects on the corrosion of magnesium. *Key Eng Mater* 2008;384:229–40.
- [18] Wang H, Estrin Y, Zúberová Z. Bio-corrosion of a magnesium alloy with different processing histories. *Mater Lett* 2008;62:2476–9.
- [19] Xin R, Wang M, Gao J, Liu P, Liu Q. Effect of microstructure and texture on corrosion resistance of magnesium alloys. *Mater Sci Forum* 2009;610–613:1160–3.
- [20] Kaesel VT, Tai PT, Bach FW, Haferkamp H, Witte F, Windhagen H. Approach to control the corrosion of magnesium by alloying. In: *Proceedings of the sixth international conference magnesium alloys and their applications*. New York: Wiley VCH, 2004. p. 534–539.
- [21] Hort N et al. Magnesium alloys as implant materials – principles of property design for Mg-RE alloys. *Acta Biomater* 2010;6:1714–25.
- [22] DiMario C et al. Drug-eluting bioabsorbable magnesium stent. *J Interv Cardiol* 2004;17(6):391–5.
- [23] Ruf J. *Organischer Metallschutz*. Hannover, Germany: Vincentz: Entwicklung und Anwendung von Beschichtungsstoffen; 1993. p. 641–5.
- [24] Ruf J. *Organischer Metallschutz*. Hannover, Germany, Vincentz: Entwicklung und Anwendung von Beschichtungsstoffen; 1993. p. 68–70.
- [25] Song G. Corrosion behavior of magnesium (Mg) alloys. In: Dong H, editor. *Surface engineering of light alloys, aluminium, magnesium, titanium alloys*. Cambridge, UK: Woodhead Publishing Ltd.; 2010. p. 3–39.
- [26] Liu Z, Gao W. Electroless nickel plating on AZ91 Mg alloy substrate. *Surf Coat Technol* 2006;200:5087–93.
- [27] Walsh FC, Low CTJ, Wood RJK, Stevens KT, Archer J, Poeton AR, et al. Review. Plasma electrolytic oxidation (PEO) for production of anodised coatings on lightweight metal (Al, Mg, Ti) alloys. *Transac Inst Met Finish* 2009;87(3):122–35.
- [28] Gnednikov SV et al. PEO coatings obtained on an Mg–Mn type alloy under unipolar and bipolar modes in silicate-containing electrolytes. *Surf Coat Technol* 2010;204:2316–22.
- [29] Gu XN, Li N, Zhou WR, Zheng YF, Zhao X, Cai QZ, et al. Corrosion resistance and surface biocompatibility of a microarc oxidation coating on a Mg–Ca alloy. *Acta Biomater* 2011;7:1880–9.
- [30] Miley HA. Fundamentals of oxidation and tarnish. In: Uhlig HH, editor. *The corrosion handbook*. New York: John Wiley; 1948. p. 11–20.
- [31] Asami K, Ono S. Quantitative X-ray photoelectron spectroscopy characterization of magnesium oxidized in air. *J Electrochem Soc* 2000;147(4):1408–13.
- [32] Santamaria M, DiQuarto F, Zanna S, Marcus P. Initial surface film on magnesium metal: a characterization by X-ray photoelectron spectroscopy (XPS) and photocurrent spectroscopy (PCS). *Electrochimica* 2007;53(3):1315–25.
- [33] Seyeux A, Liu M, Schmutz P, Song G, Atrens A, Marcus P. ToF-SIMS depth profile of the surface film on pure magnesium formed by immersion in pure water and the identification of magnesium hydride. *Corros Sci* 2009;51:1883–6.
- [34] Liu M et al. A first quantitative XPS study of the surface films formed, by exposure to water, on Mg and on the Mg–Al intermetallics: Al<sub>3</sub>Mg<sub>2</sub> and Mg<sub>17</sub>Al<sub>12</sub>. *Corros Sci* 2009;51:1115–27.
- [35] Hänzli AC, Gunde P, Schinhammer M, Uggowitzer PJ. On the biodegradation performance of an Mg–Y–RE alloy with various surface conditions in simulated body fluid. *Acta Biomater* 2009;5:162–71.
- [36] Pourbaix M. *Atlas of electrochemical equilibrium in aqueous solutions*. Oxford: Pergamon Press; 1966.
- [37] Lorenz C, Brunner JG, Kollmannsberger P, Jaafar L, Fabry B, Virtanen S. Effect of surface pre-treatments on biocompatibility of magnesium. *Acta Biomater* 2009;5:2783–9.
- [38] Fischer J, Pröfrock D, Hort N, Willumeit R, Feyerabend F. Improved cytotoxicity testing of magnesium materials. *Mater Sci Eng* 2011;B176:830–4.
- [39] Ng WF, Wong MH, Cheng FT. Stearic acid coating on magnesium for enhancing corrosion resistance in Hanks' solution. *Surf Coat Technol* 2010;204:1823–30.
- [40] Makar GL, Kruger J. Corrosion of magnesium. *Int Mater Rev* 1993;38(3):138–53.
- [41] Chen J, Wang J, Han EH, Ke W. In situ observation of pit initiation of passivated AZ91 magnesium alloy. *Corros Sci* 2009;51:477–84.
- [42] Ishizaki T, Shigematsu I, Saito N. Anticorrosive magnesium phosphate coating on AZ31 magnesium alloy. *Surf Coat Technol* 2009;203:2288–91.
- [43] Zhou W, Shan D, Han E, Ke W. Structure and formation mechanism of phosphate conversion coating on die-cast AZ91D magnesium alloy. *Corros Sci* 2008;50:329–37.
- [44] Cheng Y, Wu H, Chen Z, Wang H, Zhang Z, Wu Y. Corrosion properties of AZ31 magnesium alloy and protective effects of chemical conversion layers and anodized coatings. *Transac Nonferrous Met Soc China* 2007;17:502–8.
- [45] Li Q, Xu S, Hu J, Zhang S, Zhong X, Yang X. The effects to the structure and electrochemical behavior of zinc phosphate conversion coatings with ethanolamine on magnesium alloy AZ91D. *Electrochim Acta* 2010;55:887–94.
- [46] Niu LY, Jiang ZH, Li GY, Gu CD, Lian JS. A study and application of zinc phosphate coating on AZ91D magnesium alloy. *Surf Coat Technol* 2006;200:3021–6.

- [47] Rocca E, Juers C, Steinmetz J. Corrosion behaviour of chemical conversion treatments on as-cast Mg–Al alloys: electrochemical and non-electrochemical methods. *Corros Sci* 2010;52:2172–8.
- [48] Lan W, Sun J, Zhou A, Zhang D. Structures of zinc–manganese phosphate film and organic coating on magnesium alloys. *Mater Sci Forum* 2009;610–613:880–3.
- [49] Aal AA. Protective coating for magnesium alloy. *J Mater Sci* 2008;43:2947–54.
- [50] Zhao M, Wu S, Luo J, Fukuda Y, Nakae H. A chromium-free conversion coating of magnesium alloy by a phosphate–permanganate solution. *Surf Coat Technol* 2006;200:5407–12.
- [51] Wang J, Li D, Yu X, Jing X, Zhang M, Jiang Z. Hydrotalcite conversion coating on Mg alloy and its corrosion resistance. *J Alloy Compd* 2010;494:271–4.
- [52] Yu BL, Pan XL, Uan JY. Enhancement of corrosion resistance of Mg–9 wt.% Al–1 wt.% Zn alloy by a calcite (CaCO<sub>3</sub>) conversion hard coating. *Corros Sci* 2010;52:1874–8.
- [53] Lin JK, Uan JY. Formation of Mg, Al-hydrotalcite conversion coating on Mg alloy in aqueous HCO<sub>3</sub><sup>-</sup>/CO<sub>3</sub><sup>2-</sup> and corresponding protection against corrosion by the coating. *Corros Sci* 2009;51:1181–8.
- [54] Hamdy AS, Farahat M. Chrome-free zirconia-based protective coatings for magnesium alloys. *Surf Coat Technol* 2010;204:2834–40.
- [55] Huo H, Li Y, Wang F. Corrosion of AZ91D magnesium alloy with a chemical conversion coating and electroless nickel layer. *Corros Sci* 2004;46:1467–77.
- [56] Chen XB, Birbilis N, Abbot TB. Review of corrosion-resistant conversion coatings for magnesium and its alloys. *Corrosion* 2011;67(3):035005–1–035005–16.
- [57] Rettig R, Virtanen S. Composition of corrosion layers on magnesium rare-earth alloy in simulated body fluids. *J Biomed Mater Res Part A* 2009;85(2):359–69.
- [58] Rettig R, Virtanen S. Time-dependent electrochemical characterization of the corrosion of a magnesium rare-earth alloy in simulated body fluids. *J Biomed Mater Res Part A* 2008;85(1):167–75.
- [59] Müller L, Müller FA. Preparation of SBF with different HCO<sub>3</sub><sup>-</sup> content and its influence on the composition of biomimetic apatites. *Acta Biomater* 2006;2:181–9.
- [60] Jo JH, Hong JY, Shin KS, Kim HE, Koh YH. Enhancing biocompatibility and corrosion resistance of Mg implants via surface treatments. *J Biomater Appl* 2011. <http://dx.doi.org/10.1177/0885328211412633>.
- [61] Hiromoto S, Yamamoto A. High corrosion resistance of magnesium coated with hydroxyapatite directly synthesized in an aqueous solution. *Electrochim Acta* 2009;54:7085–93.
- [62] Gray-Munro JE, Strong M. The mechanism of deposition of calcium phosphate coatings from solution onto magnesium alloy AZ31. *J Biomed Mater Res Part A* 2009;90(2):339–50.
- [63] Chen XB, Birbilis N, Abbott TB. A simple route towards a hydroxyapatite–Mg(OH)<sub>2</sub> conversion coating for magnesium. *Corros Sci* 2011;53:2263–8.
- [64] Xu L, Pan F, Yu G, Yang L, Zhang E, Yang K. In vitro and in vivo evaluation of the surface bioactivity of a calcium phosphate coated magnesium alloy. *Biomaterials* 2009;30:1512–23.
- [65] Yang JX, Cui FZ, Lee IS, Zhang Y, Yin QS, Xia H, et al. In vivo biocompatibility and degradation behavior of Mg alloy coated by calcium phosphate in a rabbit model. *J Biomater Appl* 2011. <http://dx.doi.org/10.1177/0885328211398161>.
- [66] Carboneras M, Garcia-Alonso MC, Escudero ML. Biodegradation kinetics of modified magnesium-based materials in cell culture medium. *Corros Sci* 2011;53:1433–9.
- [67] Chiu KY, Wong MH, Cheng FT, Man HC. Characterization and corrosion studies of fluoride conversion coating on degradable Mg implants. *Surf Coat Technol* 2007;202:590–8.
- [68] Witte F, Fischer J, Nellesen J, Vogt C, Vogt J, Donath T, et al. In vivo corrosion and corrosion protection of magnesium alloy LAE442. *Acta Biomater* 2010;6:1792–9.
- [69] Seitz JM, Collier K, Wulf E, Bormann D, Bach FW. Comparison of the corrosion behavior of coated and uncoated magnesium alloys in an in vitro corrosion environment. *Adv Eng Mater* 2011;13(9):B313–23.
- [70] Supplit R, Koch T, Schubert U. Evaluation of the anti-corrosive effect of acid pickling and sol–gel coating on magnesium AZ31 alloy. *Corros Sci* 2007;49:3015–23.
- [71] Blawert C, Dietzel W, Ghali E, Song G. Anodizing treatments for magnesium alloys and their effect on corrosion resistance in various environments. *Adv Eng Mater* 2006;8(6):511–33.
- [72] Schultze JW, Lohrengel MM. Stability, reactivity and breakdown of passive films: problems of recent and future research. *Electrochim Acta* 2000;45:2499–513.
- [73] Ismail KM, Virtanen S. Electrochemical behavior of magnesium alloy AZ31 in 0.5 M KOH solution. *Electrochem Solid-State Lett* 2007;10(3):C9–C11.
- [74] Zhou X, Thompson GE, Skeldon P, Wood GC, Shimizu K, Habazaki H. Film formation and detachment during anodizing of Al–Mg alloys. *Corros Sci* 1999;41:1599–613.
- [75] Barchiche CE, Rocca E, Juers C, Hazan J, Steinmetz J. Corrosion resistance of plasma-anodized AZ91D magnesium alloy by electrochemical methods. *Electrochim Acta* 2007;53:417–25.
- [76] Barton TF. Anodization of magnesium and magnesium based alloys. US patent 005792335A, 1998, p. 5.
- [77] Kurze P. Herstellung keramischer Schichten auf Leichtmetallen mittels plasmachemischer Verfahren in Elektrolyten. *Mat-Wiss Werkstofftech* 1998;29:85–9.
- [78] Shi Z, Song G, Atrens A. Corrosion resistance of anodized single-phase Mg alloys. *Surf Coat Technol* 2006;201:492–503.
- [79] Kappell G, Kurze P, Banerjee D, Adden N. Method for producing a corrosion-inhibiting coating on an implant made of a biocorrosible magnesium alloy and implant produced according to the method. US patent 0131052A1, 2010.
- [80] Wie W, Berger S, Shrestha N, Schmuki P. Ideal hexagonal order: formation of self-organized anodic oxide nanotubes and nanopores on a Ti–35Ta Alloy. *J Electrochem Soc* 2010;157:C409–13.
- [81] Saji VS, Choe HC, Brantley WA. An electrochemical study on self-ordered nanoporous and nanotubular oxide on Ti–35Nb–5Ta–7Zr alloy for biomedical applications. *Acta Biomater* 2009;5:2303–10.
- [82] Turhan MC, Lynch RP, Jha H, Schmuki P, Virtanen S. Anodic growth of self-ordered magnesium oxy-fluoride nanoporous/tubular layers on Mg alloy (WE43). *Electrochem Commun* 2010;12:796–9.
- [83] Unceta N, Sèby F, Malherbe J, Donard OFX. Chromium speciation in solid matrices and regulation: a review. *Anal Bioanal Chem* 2010;397:1097–111.
- [84] Srinivasan PB, Liang J, Blawert C, Störmer M, Dietzel W. Characterization of calcium containing plasma electrolytic oxidation coatings on AM50 magnesium alloy. *Appl Surf Sci* 2010;256:4017–22.
- [85] Zhang XP, Zhao ZP, Wu FM, Wang YL, Wu J. Corrosion and wear resistance of AZ91D magnesium alloy with and without microarc oxidation coating in Hank's solution. *J Mater Sci* 2007;42:8523–8.
- [86] Xu X, Lu P, Guo M, Fang M. Cross-linked gelatin/nanoparticles composite coating on micro-arc oxidation film for corrosion and drug release. *Appl Surf Sci* 2010;256:2367–71.
- [87] Gao JH, Shi XY, Yang B, Hou SS, Meng EC, Guan FX, et al. Fabrication and characterization of bioactive composite coatings on Mg–Zn–Ca alloy by MAO/sol-gel. *J Mater Sci: Mater Med* 2011;22:1681–7.
- [88] Yao Z, Li L, Jiang Z. Adjustment of the ratio of Ca/P in the ceramic coating on Mg alloy by plasma electrolytic oxidation. *Appl Surf Sci* 2009;255:6724–8.
- [89] Shi P, Ng WF, Wong MH, Cheng FT. Improvement of corrosion resistance of pure magnesium in Hanks' solution by microarc oxidation with sol–gel TiO<sub>2</sub> sealing. *J Alloy Compd* 2009;469:286–92.
- [90] Wu C, Wen Z, Dai C, Lu Y, Yang F. Fabrication of calcium phosphate/chitosan on AZ91D magnesium alloy with a novel method. *Surf Coat Technol* 2010;204:3336–47.
- [91] Boccaccini AR, Keim S, Ma R, Li Y, Zhitomirsky I. Electrophoretic deposition of biomaterials. *J R Soc Interface* 2010;7(Suppl. 5):S581–613.
- [92] Liu C, Xin Y, Tian X, Chu PK. Corrosion behavior of AZ91 magnesium alloy treated by plasma immersion ion implantation and deposition in artificial physiological fluids. *Thin Solid Films* 2007;516:422–7.
- [93] Wang X, Zeng X, Wu G, Yao S, Lai Y. Effects of tantalum ion implantation on the corrosion behavior of AZ31 magnesium alloys. *J Alloy Compd* 2007;437:87–92.
- [94] Zhou H, Chen F, Yang Y, Wan H, Cai S. Study on process of ion implantation on AZ31 magnesium alloy. *Key Eng Mater* 2008;373(374):342–5.
- [95] Wu G, Zeng X, Yao S, Han H. Ion implanted AZ31 magnesium alloy. *Mater Sci Forum* 2007;546–549:551–4.
- [96] Wan YZ, Xiong GY, Luo HL, He F, Huang Y, Wang YL. Influence of zinc ion implantation on surface nanomechanical performance and corrosion resistance of biomedical magnesium–calcium alloys. *Appl Surf Sci* 2008;254:5514–6.
- [97] Wu G, Ding K, Zeng X, Wang X, Yao S. Improving corrosion resistance of titanium-coated magnesium alloy by modifying surface characteristics of magnesium alloy prior to titanium coating deposition. *Scripta Mater* 2009;61:269–72.
- [98] Fukumoto S, Sugahara K, Yamamoto A, Tsubakino H. Improvement of corrosion resistance and adhesion of coating layer for magnesium alloy coated with high purity magnesium. *Mater Transac* 2003;44(4):518–23.
- [99] Choi J, Nakao S, Kim J, Ikeyama M, Kato T. Corrosion protection of DLC coatings on magnesium alloy. *Diamond Relat Mater* 2007;16:1361–4.
- [100] Wu G, Sun L, Dai W, Song L, Wang A. Influence of interlayers on corrosion resistance of diamond-like carbon coating on magnesium alloy. *Surf Coat Technol* 2010;204:2193–6.
- [101] Nijhuis AWG, Leeuwenburgh CG, Jansen JA. Wet-chemical deposition of functional coatings for bone implantology. *Macromol Biosci* 2010;10:1316–29.
- [102] Orlowski M, Rübber A. Bioresorbable metal stents with controlled resorption. World Intellectual property organization patent WO 092436A2, 2008. p. 1–26.
- [103] Bertsch T, Borck A. Biocorrosible metallic implant having a coating or cavity filling made of gelatin. US patent 0058923A1, 2008. p. 1–3.
- [104] Borck A. Biocorrosible metallic implant having coating or cavity filling made of a PEG/PLGA copolymer. US patent 0051872A1, 2008. p. 1–3.
- [105] Adden N. Implant of a biocorrosible magnesium alloy and having a coating of a biocorrosible polyphosphazene. US patent 0048660A1, 2009. p. 1–3.
- [106] Song YW, Shan DY, Han EH. Electrodeposition of hydroxyapatite coating on AZ91D magnesium alloy for biomedical application. *Mater Lett* 2008;62:3276–9.
- [107] Wen C, Guan S, Peng L, Ren C, Wang X, Hu Z. Characterization and degradation behavior of AZ31 alloy surface modified by bone-like hydroxyapatite for implant applications. *Appl Surf Sci* 2009;255:6433–8.
- [108] Kannan MB, Orr L. In vitro mechanical integrity of hydroxyapatite coated magnesium alloy. *Biomed Mater* 2011;6:045003–11.
- [109] Feil F, Fürbeth W, Schütze M. Purely inorganic coatings based on nanoparticles for magnesium alloys. *Electrochim Acta* 2009;54:2478–86.

- [110] Zhong X, Li Q, Chen B, Wang J, Hu J, Hu W. Effect of sintering temperature on corrosion properties of sol–gel based  $\text{Al}_2\text{O}_3$  coatings on pre-treated AZ91D magnesium alloy. *Corros Sci* 2009;51:2950–8.
- [111] Lalk M, Reifenrath J, Rittershaus D, Bormann D, Meyer-Lindenberg A. Biocompatibility and degradation behaviour of degradable magnesium sponges coated with bioglass – method establishment within the framework of a pilot study. *Mat-Wiss Werkstofftech* 2010;41(12):1025–34.
- [112] Roy A, Singh S, Lee B, Ohodnicki J, Kumta PN. Novel sol–gel derived calcium phosphate coatings on Mg4Y alloy. *Mater Sci Eng* 2011;B176:1679–89.
- [113] Li JN, Cao P, Zhang XN, Zhang SX, He YH. In vitro degradation and cell attachment of a PLGA coated biodegradable Mg–6Zn based alloy. *J Mater Sci* 2010;45:6038–45.
- [114] Chen Y, Song Y, Zhang S, Li J, Zhao C, Zhang X. Interaction between a high purity magnesium surface and PCL and PLA coatings during dynamic degradation. *Biomed Mater* 2011;6:1–8.
- [115] Gu XN, Zheng YF, Lan QX, Cheng Y, Zhang ZX, Xi TF, et al. Surface modification of an Mg–1Ca alloy to slow down its biocorrosion by chitosan. *Biomed Mater* 2009;4:044109.
- [116] Wong HM, Yeung KWK, Lam KO, Tam V, Chu PK, Luk KDK, et al. A biodegradable polymer-based coating to control the performance of magnesium alloy orthopaedic implants. *Biomaterials* 2010;31:2084–96.
- [117] Hahn BD et al. Aerosol deposition of hydroxyapatite–chitosan composite coatings on biodegradable magnesium alloy. *Surf Coat Technol* 2011;205:3112–8.
- [118] Adden N, Kappelt G, Klocke B, Mueller H, Sager L. Medical implant for medicine dispersion with porous surface. EP patent 2233162, 2009.
- [119] Cohavi O et al. Protein–surface interactions: challenging experiments and computations. *J Mol Recogn* 2010;23:259–62.